Electronic Supplementary Material (ESI) for Reaction Chemistry & Engineering.

Supporting Information

Adaptive Mixed Variable Bayesian Self-Optimisation of Catalytic Reactions

*Naser Aldulaijan, Joe A. Marsden, Jamie A. Manson, Adam D. Clayton**

Contents

1 Adaptive Latent Bayesian Optimiser (ALaBO)

Bayesian optimisation commonly uses Gaussian process (GP) surrogate models to describe the relationship between the input variables and the desired response. Let $y(\cdot)$ denote the response model with inputs $w = (x, t)$, where $x = (x_1, x_2, \dots, x_p)$ represent p continuous variables, and $t = (t_1, t_2, \dots, t_q)$ represent q categorical variables, with the j th categorical variable having m_j levels, $j = 1,2, \dots, q$. For a design space with only continuous variables x, the model can be defined as:

$$y(x) = \mu + G(x) \tag{1}$$

$$K(\cdot,\cdot) = \sigma^2 R(\cdot,\cdot\,|\emptyset) \tag{2}$$

where μ is a constant prior mean and $G(x)$ is a zero-mean GP with covariance function $K(\cdot,\cdot)$, where σ^2 is the prior variance and $R(\cdot,\cdot\,|\emptyset)$ is the correlation function with $\emptyset$ correlation parameters.

The correlation function defines how similar the function values at two different points in the search space are expected to be. It measures the covariance between these points, indicating how changes in the value of one point might relate to changes in the value of another point i.e., it encodes the prior belief about the smoothness and interactions within the unknown objective function.

The Adaptive Latent Bayesian Optimiser (ALaBO) constructs a 2D latent variable (LV) representation of the categorical and continuous variables according to Apley et al.[1] For a single categorical variable (q = 1), the m levels of t are mapped to m points in 2D latent space. Therefore, the input $w = (x, t)$ is mapped to $(x, z(t))$, where $z(t)$ is a numerical vector. The corresponding Gaussian correlation function is:

$$Cor\{y(x,t), y(x',t')\} = exp\left\{-\sum_{i=1}^{p} \emptyset_i (x_i - x_i')^2 - \|z(t) - z(t')\|_2^2\right\} \tag{3}$$

When there are multiple categorical variables (q > 1), the approach scales by using a different 2D LV z^j to represent each categorical variable t_j $(j = 1,2, \dots, q)$. Here there are $2m_j - 3$ parameters for each z^j, resulting in $\sum_{j=1}^{q}(2m_j - 3)$ parameters which are estimated using maximum likelihood estimation. The corresponding Gaussian correlation function is:

$$\begin{aligned} &Cor\left\{y\left(x, t = \left(t_1, \dots, t_q\right)\right), y\left(x', t' = \left(t_1', \dots, t_q'\right)\right)\right\} \\ &\qquad = exp\left\{-\sum_{j=1}^{p} \emptyset_j \left(x_j - x_j'\right)^2 - \sum_{j=1}^{q} \left\| z^j\left(t_j\right) - z^j(t_j')\right\|_2^2\right\} \end{aligned} \tag{4}$$

The acquisition function guides the selection of the next point to evaluate in the search space. It quantifies the utility or potential benefit of evaluating a candidate point based on the surrogate model of the objective function i.e., it aims to balance the trade-off between exploration (trying new points) and exploitation (sampling where the function is likely to be optimal).

ALaBO utilises an adaptive expected improvement (AEI) acquisition function as described by Pyzer-Knapp et al.[2] For maximisation, the improvement, γ, for a given data point, x, can be defined by:

$$\gamma(x) = \frac{\mu(x) - f^*}{\sigma(x)} \tag{5}$$

where f^* is the current best observation and $\mu(x)$ is the predicted means from the model with corresponding variances, $\sigma(x)$. Expected improvement (EI) is a widely used acquisition function which simultaneously considers the probability and magnitude of improvement a data point offers over the current best point:

$$EI(x) = \mu(x) - f^*\Phi(\gamma) + \sigma(x)\emptyset(\gamma) \tag{6}$$

where Φ and $\emptyset$ are the cumulative and probability density functions respectively. In this form, EI will heavily favour exploitation over exploration of the design space, thus potentially failing to identify more lucrative solutions. This can be resolved by modification of the improvement function [Eq. (5)] to include a hyperparameter, ε, which defines the trade-off between exploitation and exploration:

$$\gamma = \frac{y_{pred} - f^* + \varepsilon}{\sigma} \tag{7}$$

where $\varepsilon \geq 0$ represents the degree of exploration. However, the requirement to predefine the value of ε is a significant limitation of this approach: if too small, the search will be highly local around the current best point; and if too large, the search will be excessively global and therefore slow to fine-tune promising solutions. AEI overcomes this limitation by allowing the trade-off parameter to dynamically change based on the current state of the model, defined as contextual improvement, χ:

$$\chi = \frac{y_{pred} - f^* + c_v}{\sigma} \tag{8}$$

$$c_v = \frac{\overline{\sigma^2}}{f^*} \tag{9}$$

where c_v is the contextual variance and $\overline{\sigma^2}$ is the mean of the variances contained in the sampled posterior distribution.

2 Simulations

2.1 Case Studies

The five case studies proposed by Jensen et al., which are based on simulated kinetic data of catalytic reactions, were used to benchmark the performance of ALaBO.[3] Each case study was designed to have unique properties by varying the kinetic parameters of three different rate equations:

$$A + B \xrightarrow{k_R} R \qquad k_R = C_{cat}^{\frac{1}{2}} A_R e^{\frac{-\left(E_{a_R} + E_{a_i}\right)}{RT}} \qquad (10)$$

$$B \xrightarrow{k_{S_1}} S_1 \qquad k_{s_1} = A_{S_1} e^{\frac{-E_{a_{S_1}}}{RT}} \qquad (11)$$

$$B + R \xrightarrow{k_{S_2}} S_2 \qquad k_{s_2} = A_{S_2} e^{\frac{-E_{a_{S_2}}}{RT}} \qquad (12)$$

where C_{A_0} = 0.167 M, C_{B_0} = 0.250 M, A_R = 3.1 × 10^7 $L^{0.5}$ $mol^{-1.5}$ s^{-1} and E_{A_R} = 55 kJ mol^{-1}.

Table S1. Overview of the settings for the five simulation case studies.

Case	Catalyst effect	k_{S_1}	k_{S_2}
1	$E_{a_1} > E_{a_{2-8}}$	= 0	= 0
2	$E_{a_1} = E_{a_2} > E_{a_{3-8}}$	= 0	= 0
3	$E_{a_1} > E_{a_{2-8}}$	> 0[a]	= 0
4	$E_{a_1} > E_{a_{2-8}}$	= 0	> 0[b]
5	$E_{a_1} > E_{a_{2-8}}\ if\ T\ < 80\ °C$	= 0	= 0

a: $E_{a_{S_1}}$ = 100 kJ mol^{-1}, A_{S_1} = 1 × 10^{12} s^{-1}
b: $E_{a_{S_2}}$ = 50 kJ mol^{-1}, A_{S_2} = 3.1 × 10^5 $L^{0.5}$ $mol^{-1.5}$ s^{-1}

Table S2. Catalyst-specific activation energies, E_{a_i} (kJ mol^{-1}), for each case study.

Catalyst	Case 1	Case 2	Case 3/4	Case 5
1 (T < 80 °C)	0	0	0	-5.0
1 (T > 80 °C)	0	0	0	-5.0 + 0.3 (T – 80)
2	0.3	0	0.3	0.7
3	0.3	0.3	0.3	0.7
4	0.7	0.7	0.7	0.7
5	0.7	0.7	0.7	0.7
6	2.2	2.2	2.2	2.2
7	3.8	3.8	3.8	3.8
8	7.3	7.3	7.3	7.3

Each case study was optimised using the catalyst type, residence time (t_{res}), temperature (T) and catalyst concentration (C_{cat}) as input variables. In contrast to the original paper, the objective was to maximise a weighted objective function, $f(x)$, combining the yield and TON with respect to desired product, *R*:

$$\begin{aligned} max \quad & f(x) \\ s.t. \quad & 1 \leq t_{res}\,(\text{min}) \leq 10 \\ & 30 \leq T(°\text{C}) \leq 110 \\ & 0.5 \leq C_{cat}\,(\text{mol}\%) \leq 2.5 \\ & \text{Cat.}\{1,2,3,4,5,6,7,8\} \end{aligned} \qquad (13)$$

$$f(x) = 0.75\ln(yield) + 0.25\ln(TON) \qquad (14)$$

To evaluate the accuracy of the optimisation algorithms the true optima for each case study were required. These were identified by performing global SNOBFIT optimisations of the continuous variables (100 iterations) for each catalyst type per case study (Table S3). The relative weightings were selected such that the optimal yield and TON were comparable with the original case studies.[3]

Table S3. Optimal solutions for each catalyst type for the five case studies.

Case —	$Cat.$ —	t_{res} (min)	T (°C)	C_{cat} (mol%)	Yield (%)	TON —	$f(x)$ —
1	1	10.0	110.0	0.500	90.4	180.8	4.6775
	2	10.0	110.0	0.500	88.8	177.6	4.6597
	3	10.0	110.0	0.500	88.8	177.6	4.6597
	4	10.0	110.0	0.500	86.5	172.9	4.6330
	5	10.0	110.0	0.500	86.5	172.9	4.6330
	6	10.0	110.0	0.500	75.7	151.4	4.5003
	7	10.0	110.0	0.500	61.8	123.6	4.2973
	8	10.0	110.0	2.500	53.2	21.3	3.7455
2	1	10.0	110.0	0.500	90.4	180.8	4.6775
	2	10.0	110.0	0.500	90.4	180.8	4.6775
	3	10.0	110.0	0.500	88.8	177.6	4.6597
	4	10.0	110.0	0.500	86.5	172.9	4.6330
	5	10.0	110.0	0.500	86.5	172.9	4.6330
	6	10.0	110.0	0.500	75.7	151.4	4.5003
	7	10.0	110.0	0.500	61.8	123.6	4.2973
	8	10.0	110.0	2.500	53.2	21.3	3.7455
3	1	10.0	81.9	1.522	54.9	36.1	3.9012
	2	10.0	81.9	1.855	54.9	29.6	3.8504
	3	10.0	81.9	1.862	54.9	29.5	3.8504
	4	10.0	82.0	2.435	54.9	22.5	3.7827
	5	10.0	82.0	2.436	54.9	22.5	3.7827
	6	10.0	83.0	2.500	41.7	16.7	3.5008
	7	10.0	83.9	2.500	29.0	11.6	3.1391
	8	10.0	85.6	2.500	11.1	4.4	2.1784
4	1	2.2	110.0	1.380	36.8	26.6	3.5243
	2	2.2	110.0	1.672	36.8	22.0	3.4772
	3	2.2	110.0	1.669	36.8	22.0	3.4772
	4	2.2	110.0	2.148	36.8	17.1	3.4144
	5	2.2	110.0	2.149	36.8	17.1	3.4144
	6	2.5	110.0	2.500	29.8	11.9	3.1661
	7	2.9	110.0	2.500	22.0	8.8	2.8618
	8	3.8	110.0	2.500	9.9	4.0	2.0669
5	1	10.0	80.0	0.500	93.8	187.5	4.7141
	2	10.0	110.0	0.500	86.5	172.9	4.6330
	3	10.0	110.0	0.500	86.5	172.9	4.6330
	4	10.0	110.0	0.500	86.5	172.9	4.6330
	5	10.0	110.0	0.500	86.5	172.9	4.6330
	6	10.0	110.0	0.500	75.7	151.4	4.5003
	7	10.0	110.0	0.500	61.8	123.6	4.2973
	8	10.0	110.0	2.500	53.2	21.3	3.7455

2.2 Simulation Procedure

The simulations were programmed in MATLAB and followed the procedure shown in Figure S1. In this work, the performance of different algorithms (ALaBO, Dragonfly, ProcessOptimizer), initialisation strategies (CP, LHC = 3, 5) and batch sizes (BS = 1, 2, 3, 4) across each of the five case studies were assessed. Therefore, each of these parameters were set as a user input prior to the start of the simulation. Each simulation was run 10 times with an experimental budget of 100, enabling the average speed of convergence and robustness of each strategy to be determined. Two-way integration of MATLAB (2023a) and Python (3.10) enabled Dragonfly and ProcessOptimizer to be called directly from MATLAB to suggest new sampling points.

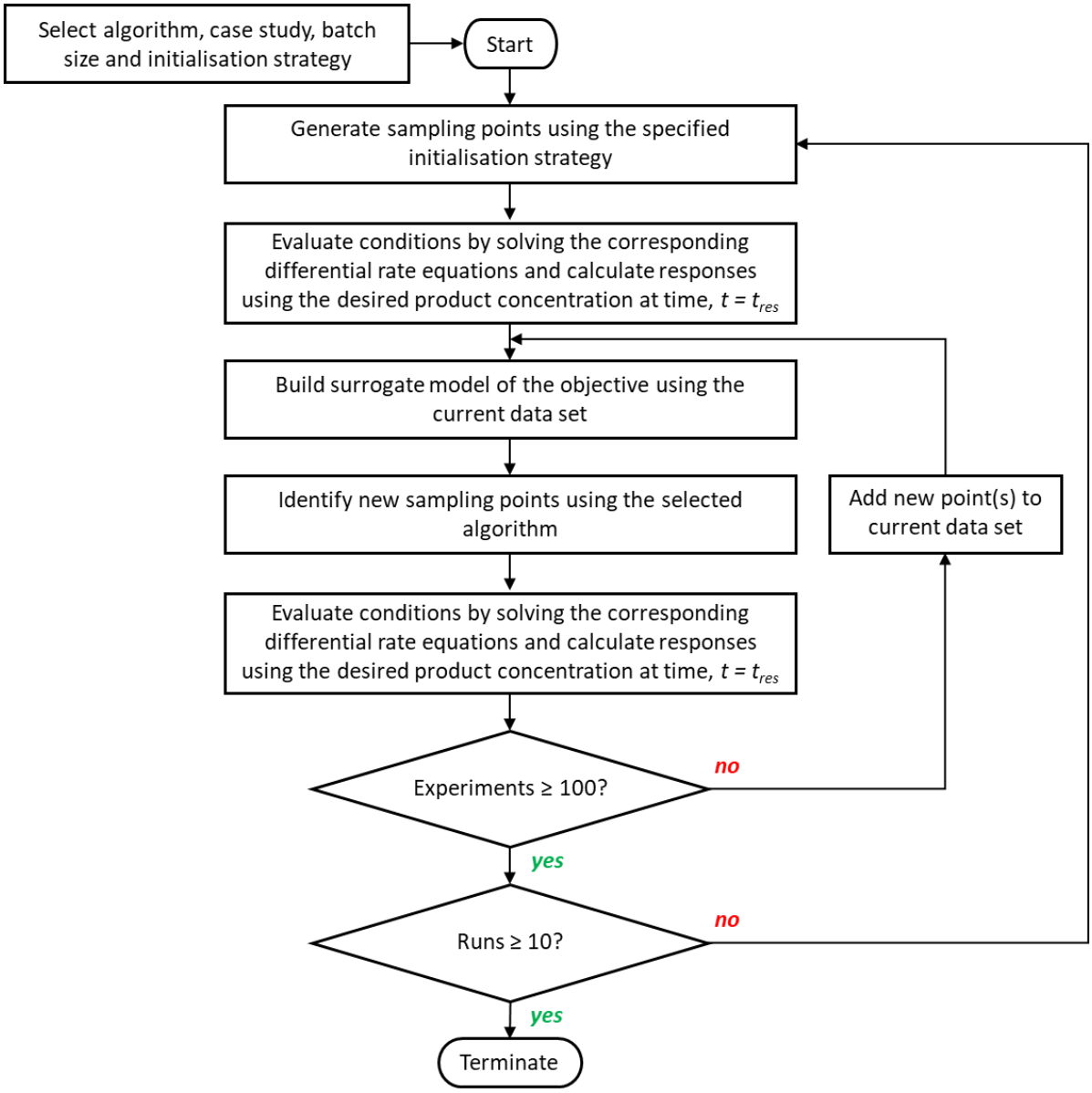

Figure S1. Flowchart of the simulated optimisations procedure.

Differential rate equations, describing the change in concentration of each compound as a function of time [Eq. (15-20)], were solved using Ordinary Differential Equation (ODE) solver ODE45. The yield and TON were calculated according to [Eq. (21)] and [Eq. (22)] respectively, where $[R]_{t_{res}}$ is the concentration of desired product at time $t = t_{res}$.

$$\frac{dC_{cat}}{dt} = 0 \tag{15}$$

$$\frac{d[A]}{dt} = -k_R[A][B] \tag{16}$$

$$\frac{d[B]}{dt} = -k_R[A][B] - k_{S_1}[B] - k_{S_2}[B][R] \tag{17}$$

$$\frac{d[R]}{dt} = k_R[A][B] - k_{S_2}[B][R] \tag{18}$$

$$\frac{d[S_1]}{dt} = k_{S_1}[B] \tag{19}$$

$$\frac{d[S_2]}{dt} = k_{S_2}[B][R] \tag{20}$$

$$Yield = \frac{[R]_{t_{res}}}{C_{A_0}} \times 100 \tag{21}$$

$$TON = \frac{[R]_{t_{res}}}{C_{cat}} \tag{22}$$

To enable the behaviour of the algorithms to be better understood, the evaluated conditions were stored alongside the responses for post-processing. These could then be used to visualise the optimisation pathway with respect to the response and each individual variable. An example of this for a run of ALaBO on case study one is shown in Figure S2.

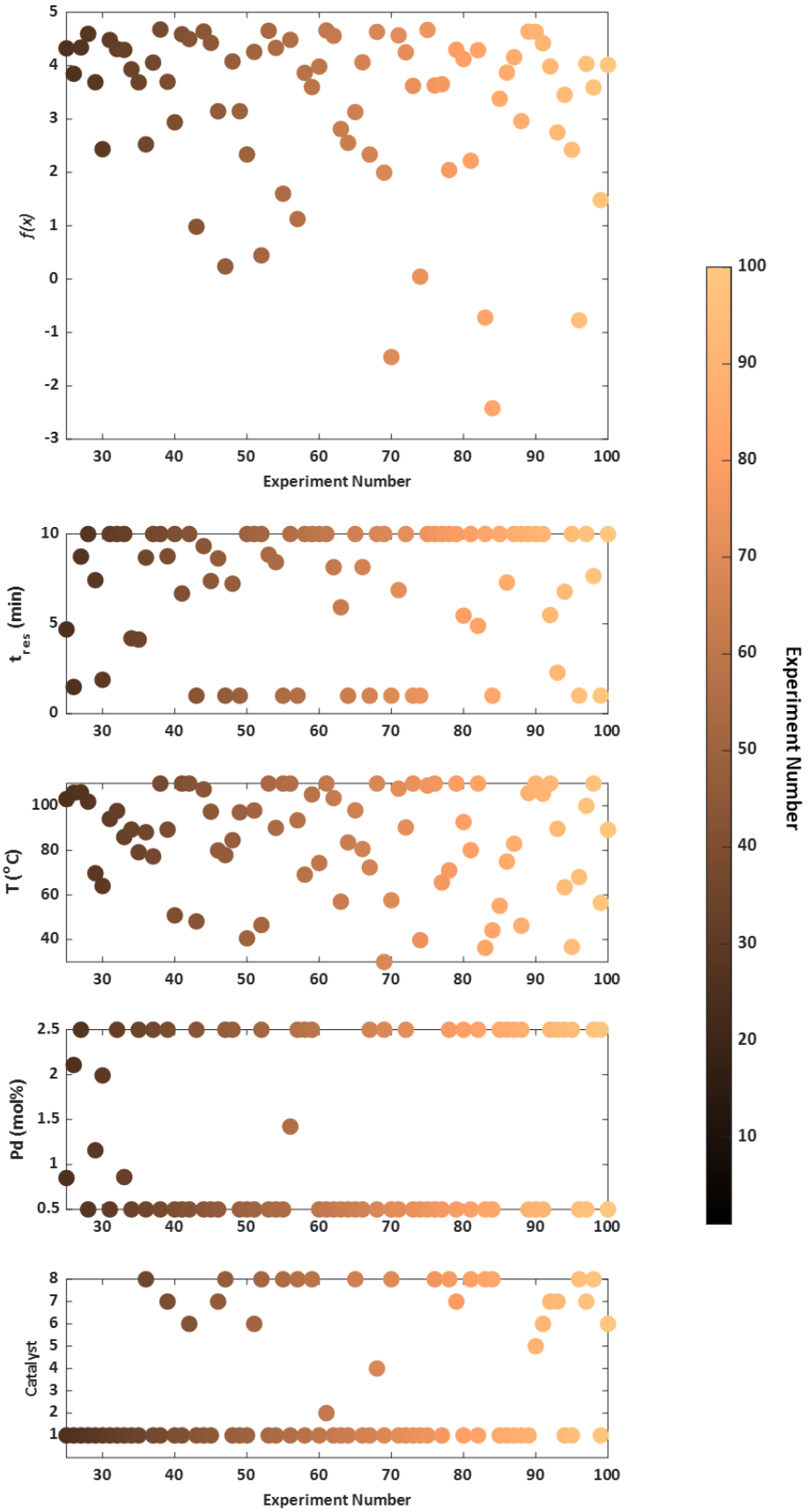

Figure S2. An example of an optimisation pathway for the objective function and each reaction variable (ALaBO, Case 1).

2.3 Results

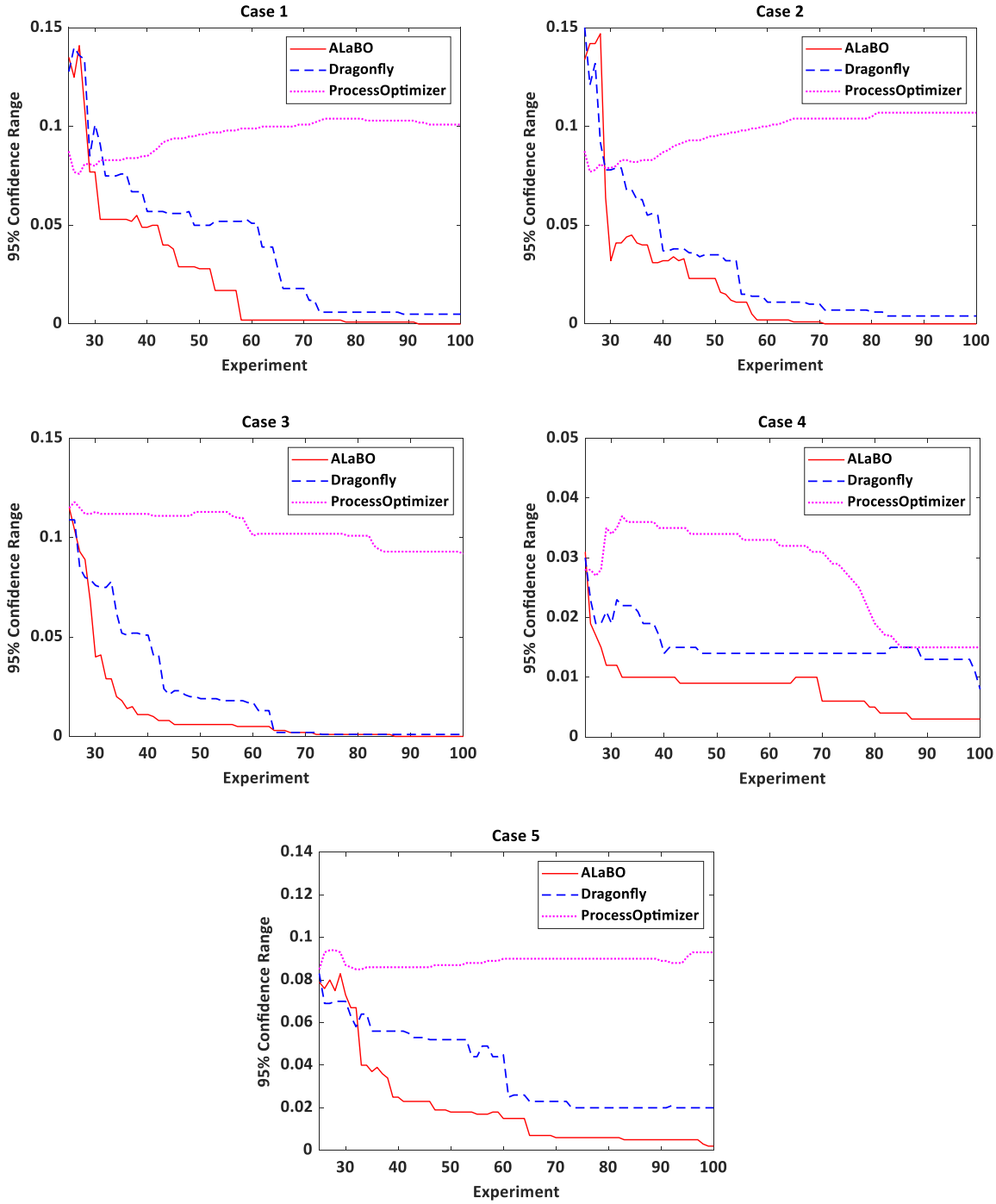

Figure S3. Robustness plots showing the evolving fragility of the model. Lower values for the 95% confidence range indicate a more reliable model at any given experiment.

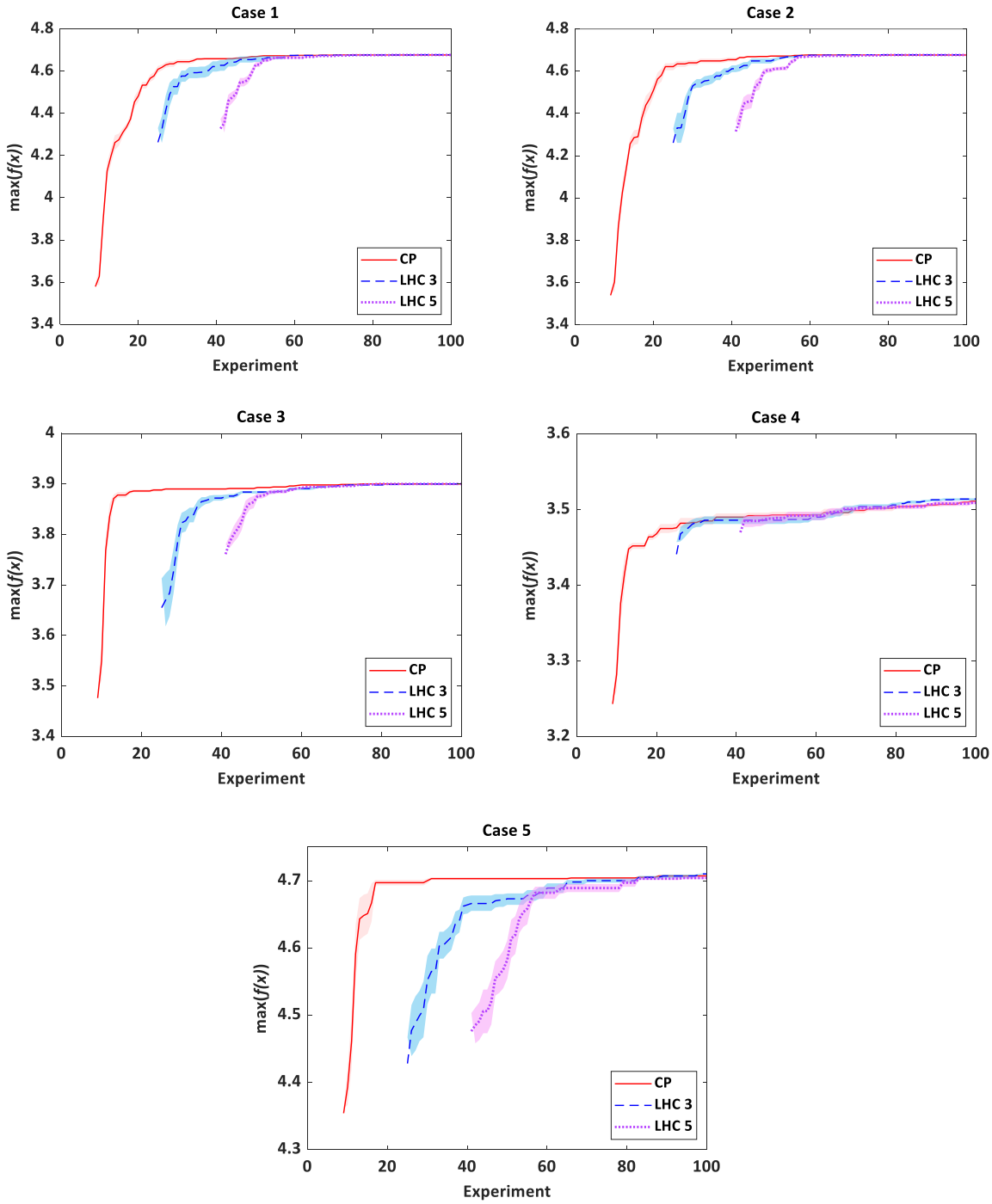

Figure S4. Optimisation progress plots comparing ALaBO performance using different initialisation strategies. Plots show the average running maxima and 95% confidence intervals across 10 separate runs. CP = centre point; LHC = Latin hypercube.

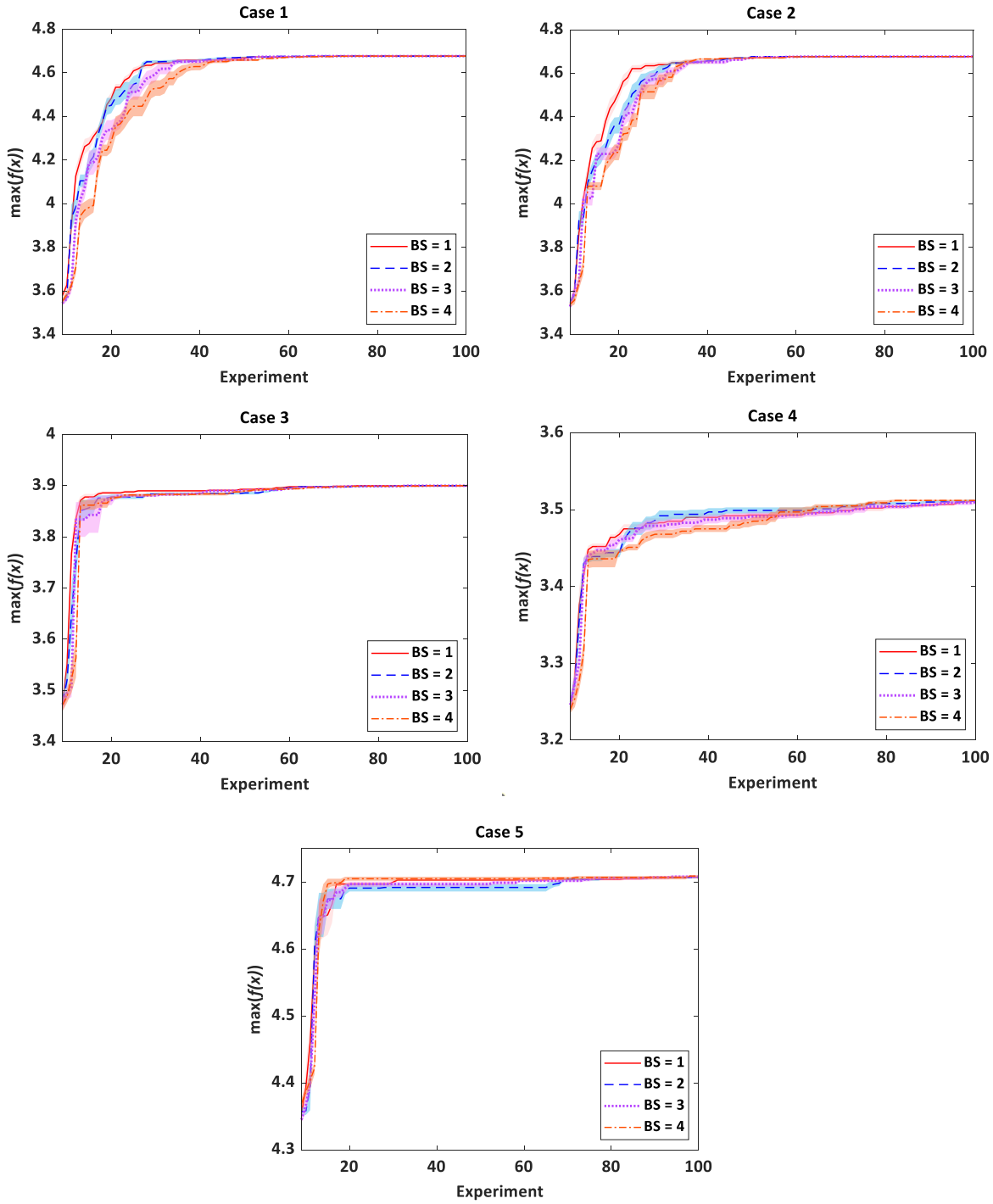

Figure S5. Optimisation progress plots comparing ALaBO performance using different iteration batch sizes (BS). Plots show the average running maxima and 95% confidence intervals across 10 runs using CP initialisation.

3 Self-Optimisation of a Suzuki-Miyaura Cross-Coupling

3.1 Automated Continuous Flow Reactor

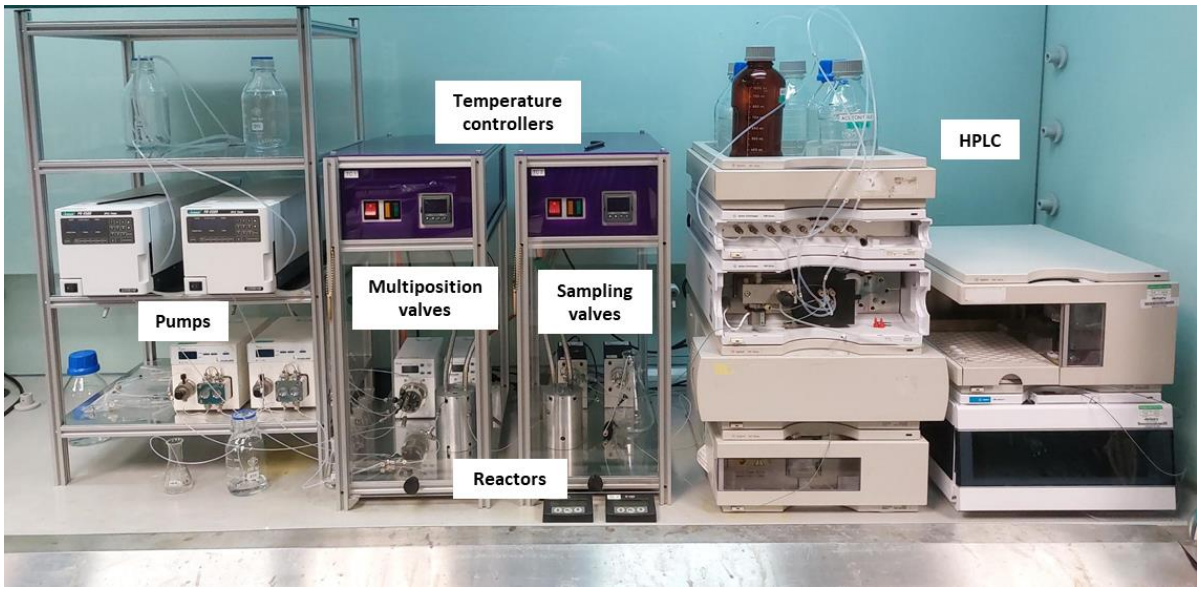

Figure S6. Photo of the automated continuous flow reactor platform.

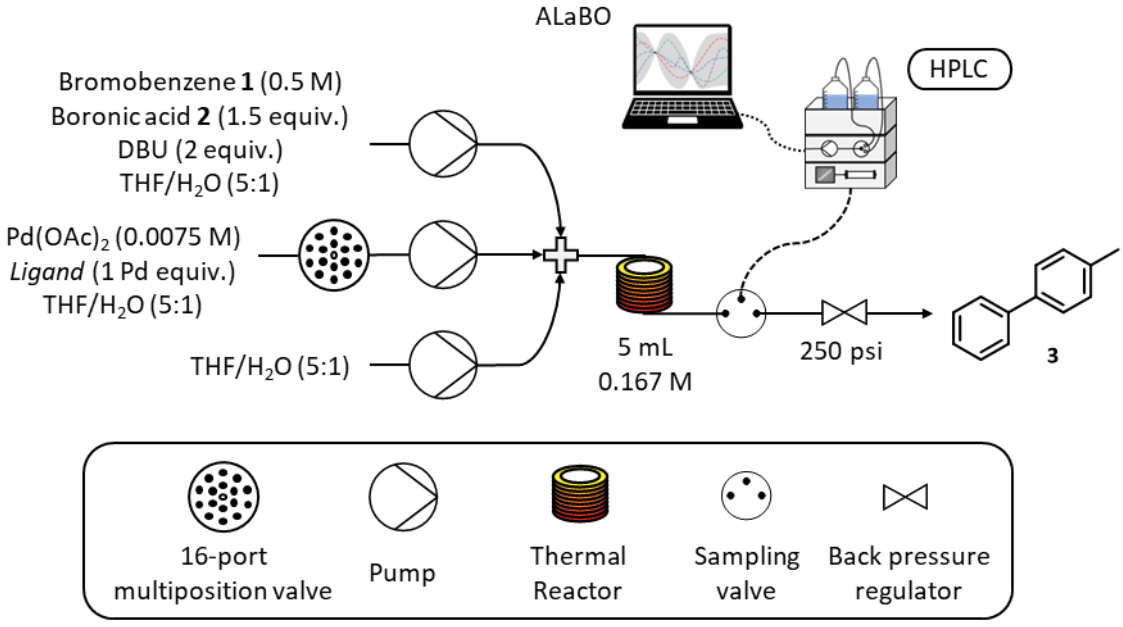

Scheme S1. Schematic of the reactor set-up for the self-optimisation of the Suzuki-Miyaura cross-coupling reaction.

Ligand selection was achieved using a Knauer Azura 16-port multiposition valve connected to a pre-prepared array of catalyst/ligand stock solutions stored under nitrogen. Reagents were pumped using a combination of JASCO (PU-4580) and Knauer Azura (P 4.1S) HPLC pumps and mixed using Swagelok SS-100-3 tee pieces. A 5 mL reactor was made from stainless steel tubing (1/16" OD, 1/32" ID), which was fitted to an aluminium cylinder and heated with a Eurotherm 3200 temperature controller. The reactor was maintained under 250 psi using an Upchurch Scientific back pressure regulator. Online HPLC sampling was achieved using a VICI Valco EUHA-CI4W sample loop (4-port) with 0.1 µL direct injection volume. Quantitative analysis was performed on an Agilent 1100 series HPLC instrument fitted with a Supelco Ascentis Express C18 reverse phase column (5 cm length, 4.6 mm ID and 2.7 µm particle size) and an Agilent EC-C18 (4.6 × 5 mm, 2.7 µm) guard column. The platform was controlled and automated using a custom written MATLAB program.

3.2 Chemicals & Analytical Method

All of the following chemicals were purchased from commercial sources and used as received: bromobenzene (98.0%, Fluorochem); 4-methylphenylboronic acid (>97%, Apollo Scientific); DBU (98.0%, Fluorochem); palladium (II) acetate (≥99.9%, Sigma-Aldrich); DavePhos (98.0%, Fluorochem); XPhos (98.0%, Fluorochem); SPhos (98.0%, Fluorochem); CyJohnPhos (99.0%, Fluorochem); dppp (95.0%, Fluorochem); dppf (97%, Sigma-Aldrich); 4-methylbiphenyl (98.0%, Fluorochem); 4,4'-dimethylbiphenyl (98%, Activate Scientific); toluene (≥99.8%, Fisher Scientific); biphenyl (99.5%, Sigma-Aldrich); tetrahydrofuran (≥99.8%, Fisher Scientific); acetonitrile (≥99.9%, Sigma-Aldrich).

Reservoir solutions were prepared by dissolving the desired reagents in solvent under nitrogen, and were replenished as required throughout the optimisation. Reagent pump (150 mL): bromobenzene **1** (7.85 mL, 0.075 mol, 0.50 M), 4-methylphenylboronic acid **2** (15.30 g, 0.113 mol, 0.75 M), DBU (22.43 mL, 0.150 mol, 1.00 M) and biphenyl (1.39 g, 0.009 mol, 0.06 M) in THF/H_2O (5:1). Catalyst pump (25 mL): $Pd(OAc)_2$ (42.1 mg, 0.0002 mol, 0.0075 M) and ligand (0.0002 mol, 0.0075 M) in THF/H_2O (5:1). Solvent pump: THF/H_2O (5:1). The catalyst pump was connected to a multiposition valve, enabling selection of six different ligands (DavePhos, XPhos, SPhos, CyJohnPhos, dppp, dppf) from separate reservoir solutions. The solvent pump was necessary to enable residence time and catalyst mol% to be varied independently whilst holding the concentration of the limiting reactant (bromobenzene **1**) fixed at 0.167 M within the reactor.

HPLC method development and analytical calibrations were performed using the products from commercial sources and biphenyl as internal standard. HPLC mobile phases were **A** H_2O (18.2 MΩ) and **B** MeCN. The method used was 5% **B** 2 min, 5 to 95% **B** 5 min, 95% **B** 1 min, 95 to 5% **B** 0.5 min, 5% **B** 1 min, flow rate 1.5 mL min^{-1}, column temperature 30 °C. An example of a HPLC chromatogram from the calibrations is shown in Figure S7. Retention times: DBU (1.30 min), 4-methylphenylboronic acid **2** (3.92 min), toluene (5.41 min), bromobenzene **1** (5.53 min), biphenyl (6.08 min), 4-methylbiphenyl **3** (6.40 min), 4,4'dimethylbiphenyl (6.70 min). Toluene and 4,4'-dimethylbiphenyl were included in HPLC method development to enable monitoring of potential protodeboronation or homocoupling reactions of 4-

methylphenylboronic acid **2**. However, these were not observed in the subsequent optimisation experiments.

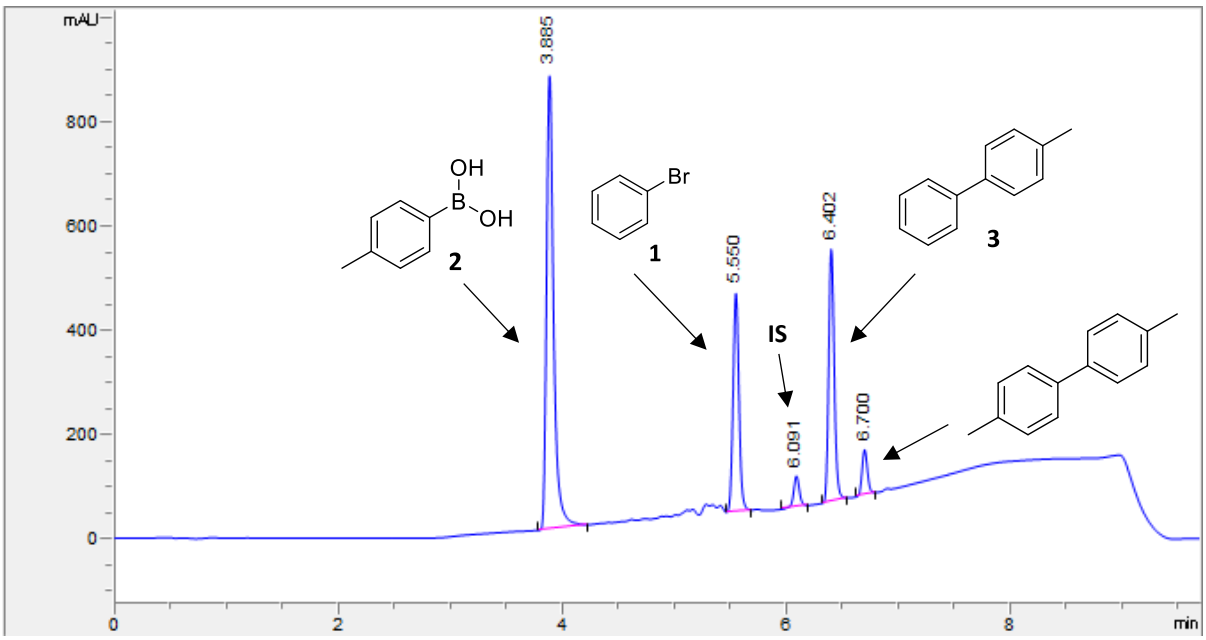

Figure S7. Example HPLC chromatogram (wavelength = 220 nm). IS = internal standard (biphenyl).

3.3 Optimisation Procedure

A custom written MATLAB program controlled the pump flow rates, valve positions, reactor temperature and sampling. Each iteration adhered to the following sequence: (i) multiposition valve was set to the corresponding ligand; (ii) reactor was allowed to stabilise at the desired operating temperature (iii) pumps were set to the required flow rates and left for three reactor volumes to reach steady state; (iv) sampling valve was triggered alongside HPLC analysis. During the analysis, the reagent pumps were paused to reduce material consumption, and the solvent pump set to 0.5 mL min^{-1} to wash the reactor. In addition, the temperature of the reactor was set to the minimum bounds. As cooling is slower than heating in this system, this provided the most time-efficient method for changing the temperature between experiments. The response was calculated from the HPLC chromatograms at the end of each iteration, and the results used to update the surrogate models and generate the next recommended reaction conditions.

The ALaBO algorithm was initialised using one centre point experiment with respect to the quantitative variables per ligand, equalling six total experiments. The optimisation was performed with a batch size of one. This process was repeated iteratively with a total experimental budget (including initialisation) of 25, after which point the optimisation was terminated.

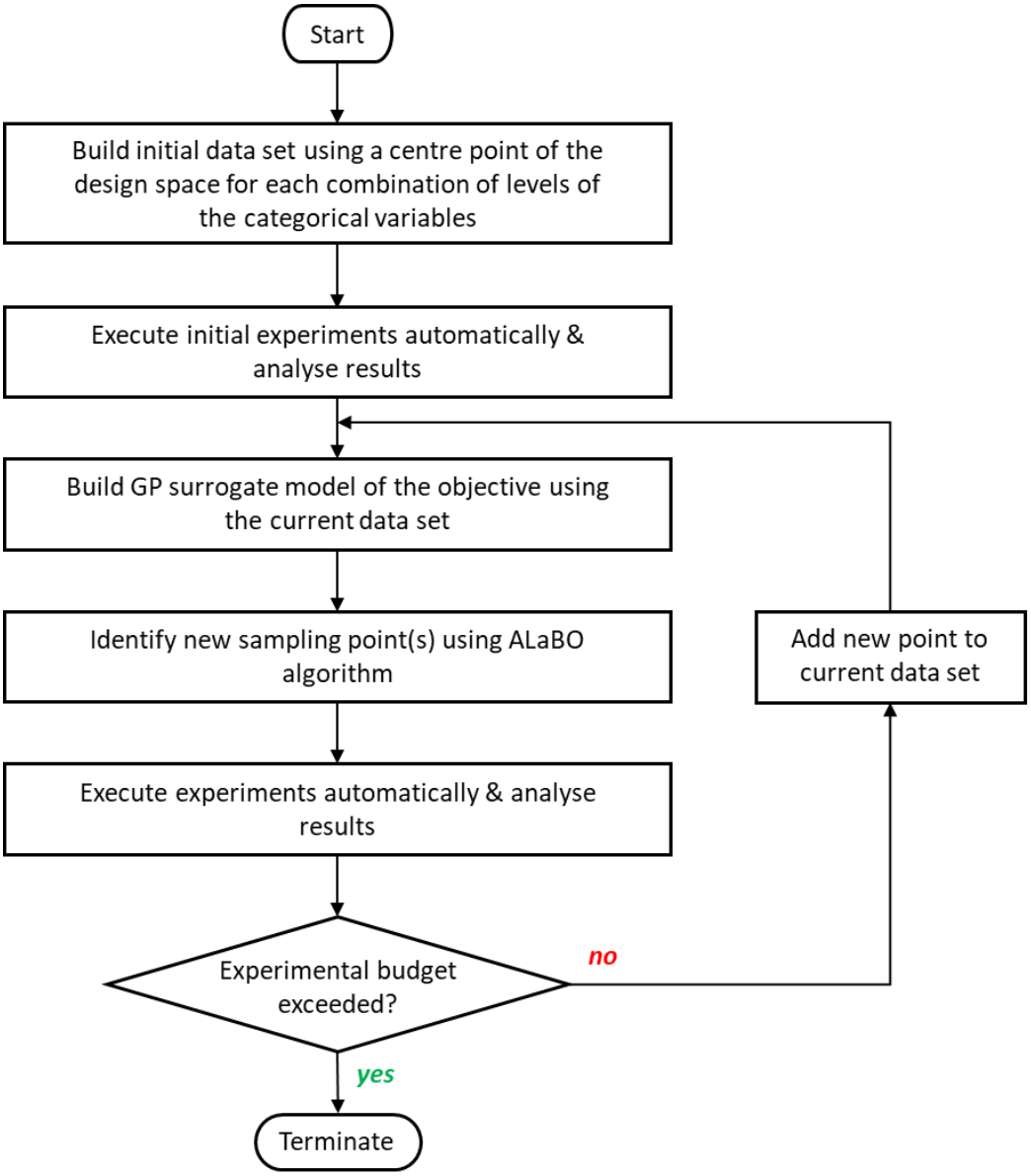

Figure S8. Flowchart of the self-optimisation experimental procedure.

The self-optimisation was conducted with respect to four variables: residence time, Pd mol%, temperature and ligand. The lower and upper bounds of the continuous variables, and the levels of the categorical variable are shown in Scheme S2. Fixed parameters were the concentration of bromobenzene **1** in the reaction (0.167 M), the equivalents of DBU and boronic acid **2** (2.0 and 1.5 respectively), and the Pd/ligand ratio (1:1). The objective of the optimisation was to simultaneously maximise the yield and TON as defined by the weighted objective function, $f(x)$ [Eq. (14)]. For reactions with a 0% yield, a value of 0.1 was assigned to the product peak area. This prevented the code from attempting to take the natural log of 0 and pass the algorithm an undefined number. However, this method still provided a poor response to deter the algorithm from further exploring this region.

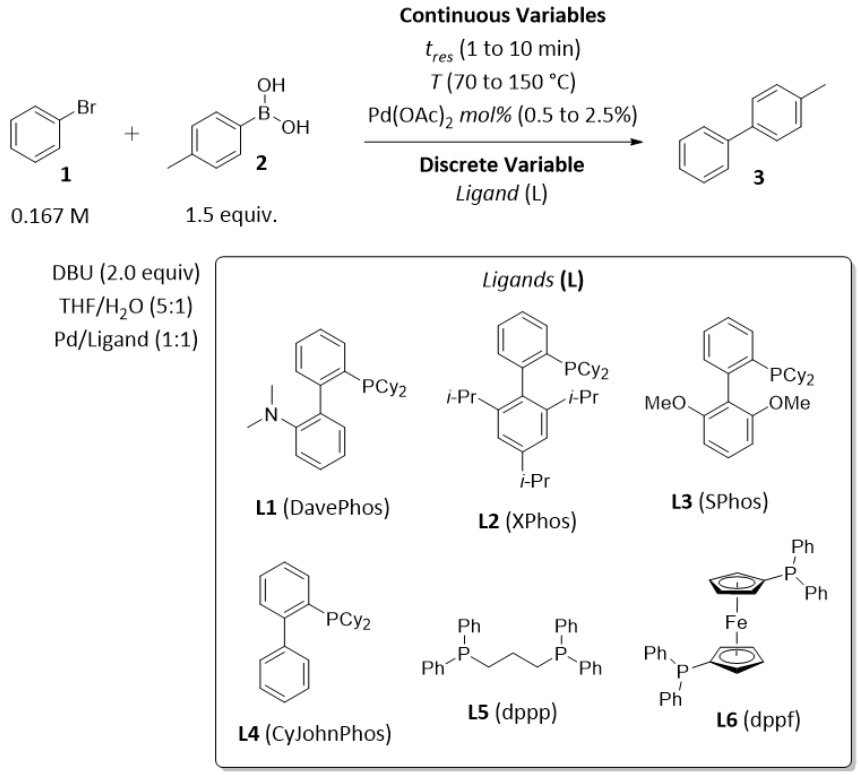

Scheme S2. Optimisation parameters for the Suzuki-Miyaura cross-coupling reaction between bromobenzene **1** and 4-methylphenylboronic acid **2**.

3.4 Results

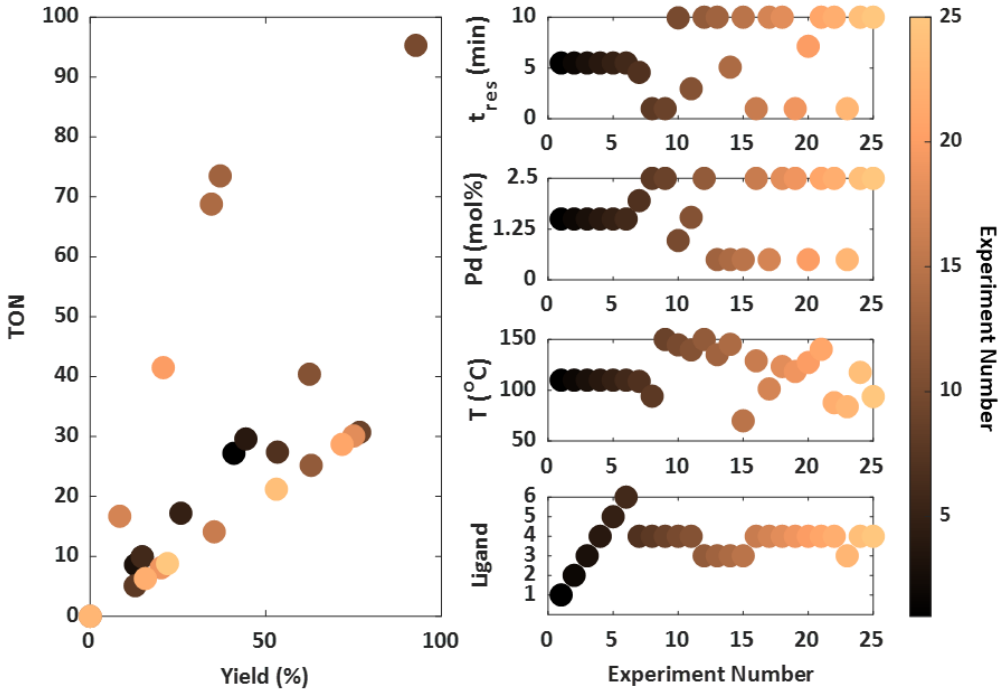

Figure S9. Optimisation pathway for the separate terms in the weighted objective function and for each reaction variable.

Table S4. Optimisation results showing the yield and TON with respect to desired product **3**, and the response from the weighted objective function. Experiments 1-6 = CP initialisation; experiments 7-25 = ALaBO iterations.

Entry	t_{res} (min)	Pd mol%	T (°C)	Ligand	Yield (%)	TON	$f(x)$
1	5.50	1.50	110.0	DavePhos	40.9	27.2	3.6085
2	5.50	1.50	110.0	XPhos	14.8	9.9	2.5921
3	5.50	1.50	110.0	SPhos	12.9	8.6	2.4570
4	5.50	1.50	110.0	CyJohnPhos	44.3	29.6	3.6906
5	5.50	1.50	110.0	dppp	25.8	17.2	3.1489
6	5.50	1.50	110.0	dppf	14.8	9.9	2.5944
7	4.57	1.95	108.8	CyJohnPhos	53.3	27.4	3.8096
8	1.00	2.50	94.2	CyJohnPhos	12.8	5.1	2.3227
9	1.00	2.50	150.0	CyJohnPhos	76.7	30.7	4.1108
10	9.94	0.97	144.7	CyJohnPhos	92.7	95.3	4.5362
11	2.96	1.54	139.7	CyJohnPhos	62.4	40.4	4.0244
12	10.00	2.50	150.0	SPhos	62.9	25.2	3.9130
13	10.00	0.50	135.1	SPhos	37.0	73.5	3.7822
14	5.08	0.50	145.2	SPhos	34.5	68.8	3.7138
15	10.00	0.50	70.0	SPhos	0.0	0.0	-5.4334
16	1.00	2.50	129.0	CyJohnPhos	35.3	14.1	3.3348
17	10.00	0.50	101.4	CyJohnPhos	8.4	16.7	2.2995
18	10.00	2.50	123.4	CyJohnPhos	75.0	30.1	4.0892
19	1.00	2.50	118.5	CyJohnPhos	20.2	8.1	2.7781
20	7.14	0.50	127.3	CyJohnPhos	20.8	41.5	3.2068
21	10.00	2.50	140.3	CyJohnPhos	71.7	28.7	4.0444
22	10.00	2.50	87.8	CyJohnPhos	15.7	6.3	2.5250
23	1.00	0.50	83.8	SPhos	0.0	0.0	-5.0861
24	10.00	2.50	117.6	CyJohnPhos	53.0	21.2	3.7420
25	10.00	2.50	93.8	CyJohnPhos	22.0	8.8	2.8613

4 References

1 Y. Zhang, S. Tao, W. Chen and D. W. Apley, *Technometrics*, 2020, **62**, 291.

2 D. Jasrasaria and E. O. Pyzer-Knapp, *arXiv.org*, 2018, 1807.01279.

3 L. M. Baumgartner, C. W. Coley, B. J. Reizman, K. W. Gao and K. F. Jensen, *React. Chem. Eng.*, 2018, **3**, 301.